International Journal of Electrical and Computer Engineering (IJECE)
Vol. 14, No. 4, August 2024, pp. 3995~4004
ISSN: 2088-8708, DOI: 10.11591/ijece.v14i4.pp3995-4004

Brain tumor detection using a MobileNetV2-SSD model with modified feature pyramid network levels

Nada Fitrieyatul Hikmah[1], Ariq Dreiki Hajjanto[1], Armand Faris A. Surbakti[1], Nadhira Anindyafitri Prakosa[1], Talitha Asmaria[2], Tri Arief Sardjono[1]
[1]Department of Biomedical Engineering, Institut Teknologi Sepuluh Nopember, Surabaya, Indonesia
[2]Center for Biomedical Research, National Research and Innovation Agency, Bogor, Indonesia

Article Info

Article history:

Received Jan 18, 2024
Revised Mar 20, 2024
Accepted Apr 30, 2024

Keywords:

Convolutional neural network
Feature pyramid network
MobileNet
Single shot MultiBox detector
Tumor

ABSTRACT

Brain tumors, a subset of these malignancies, demand accurate and efficient diagnosis. Traditional methods use non-invasive medical imaging like magnetic resonance imaging (MRI) and computed tomography (CT). Although necessary for diagnosis, manual brain MRI picture segmentation is tedious and time-consuming. Using deep learning is a promising solution. This study proposes an innovative approach for brain tumor detection, focusing on meningioma tumors. Utilizing threshold-based segmentation, the MobileNetV2 architecture, a modified feature pyramid network (FPN), and single shot MultiBox detector (SSD), our model achieves precise localization and object detection. Pre-processing techniques such as grayscale conversion, histogram equalization, and Gaussian filtering enhance the MRI image quality. Morphological operations and thresholding facilitate tumor segmentation. Data augmentation and a meticulous dataset division aid in model generalization. The architecture combines MobileNetV2 as a feature extractor, SSD for object detection, and FPN for detecting small objects. Modifications, including lowering the minimum FPN level, enhance small object detection accuracy. The proposed model achieved a recall value of around 98% and a precision value of around 89%. Additionally, the proposed model achieved approximately 93% on both the dice similarity coefficient (DSC) value and the index of similarity. Based on the promising results, our research holds significant advancements for the field of medical imaging and tumor detection.

Corresponding Author:

Nada Fitrieyatul Hikmah
Department of Biomedical Engineering, Institut Teknologi Sepuluh Nopember
Jalan Teknik Kimia, Keputih, Kec. Sukolilo, Surabaya, East Java 60111, Indonesia
Email: nadafh@bme.its.ac.id

1. INTRODUCTION

Cancer orchestrates a severe and potentially fatal group of diseases that can originate in virtually any organ or tissue within the body. This occurs when abnormal cells begin to multiply in an uncontrollable and rapid manner. The World Health Organization (WHO) identifies cancer as the world's second most common cause of death, responsible for approximately 9.6 million deaths, which represents one out of every six deaths [1]. A brain tumor refers to a collection of abnormal cells within the brain, which can either be malignant (cancerous) or benign (non-cancerous). During the past decade, more than a hundred types of brain tumors were discovered by medical experts and neuroscientists. These brain tumors can be grouped into two main categories, which are primary brain tumors, which originate from the brain, and secondary brain deposits, where the primary tumor does not originate in the brain and is somewhere else in the body [2].

Normally, non-invasive medical imaging techniques and methods such as magnetic resonance imaging (MRI) and computer tomography (CT) are chosen as brain tumor identification tools over invasive procedures such as tissue biopsies [3]. Overall, alternative medical-image-based diagnosis techniques are recommended in the contemporary medical care system. It is a laborious and time-consuming process to manually segment and analyze structural MRI images in order to detect brain tumors. At present, it remains within the purview of certified radiologists, exclusively [4]. In the extraction of brain MRI images, radiologists apply manual segmentation techniques, leveraging previous records from MRI images that include anatomical and physiological characteristics. The main challenge is that the segmentation of brain MRI needs domain expertise to avoid fatal human errors [5]. Since the objective is to obtain the result of the segmentation of brain tumors from many patients, an advanced and robust alternative brain tumor segmentation will have a substantial impact on brain tumor diagnosis and treatment [6]. Artificial intelligence (AI) brought human biological neural networks in the form of computational models, significantly improving the decision-making process's efficiency [5], [7]. Deep learning (DL) is one of AI's most groundbreaking advancements. Among DL models, the convolutional neural network (CNN), utilizes different convolutional layers to extract features from images for visual recognition, such as object detection, classification, and, most importantly, brain segmentation [8].

When applied to brain tumor segmentation, deep learning methods extract important and crucial features automatically. In the context of transfer learning (TL), Swati *et al.* [9] showcased a method of brain tumor classification using DL and TL. This method could maximize the extraction of significant features from MRI images and subsequently could facilitate the classification of brain tumors based on the MRI images. Fine-tuning was applied to improve accuracy rates. Additionally, a research study proposed by Sadrawi *et al.* [10] examined various CNN models for their effectiveness in identifying brain tumors, which generally achieved satisfactory results, although it primarily used more distinct images, which facilitated detection and led to better outcomes. However, detecting smaller images, which may contain subtler or less conspicuous tumor features, could present a challenge for the models evaluated in this study. He *et al.* [11] employed a semantic feature pyramid network (FPN) transformer for cancer detection, which could potentially address the challenge of identifying smaller images. However, this approach utilized a transformer attention mechanism which attained significant computational complexity and resource requirements, and the study was tested on a breast tumor dataset rather than a brain tumor dataset.

Conventional brain tumor detection methods often require extensive resources for model training. Additionally, the MRI dataset by Cheng [12] poses a significant challenge for CNNs due to its small size compared to other public datasets. Therefore, this study explored the landscape of brain tumor detection by integrating various segmentation techniques and localization methods through the MobileNet V2-SSD architecture with a modified FPN level. The modification involved lowering the FPN level to capture more detailed features, enabling the detection of even small brain tumors.

The layout of this paper is organized as follows: section 1 provides a comprehensive introduction, outlining the significance of brain tumor detection and the challenges faced. Section 2 delves into different methodologies, including pre-processing, segmentation, and object detection techniques. Section 3 presents the results of the experiment and discusses them. Finally, the paper concludes in the last section, summarizing the discoveries and suggesting potential improvements for future research.

2. RESEARCH METHOD

In this section, a novel approach for brain tumor localization and detection is presented, which utilizes several different combinations of advanced techniques, including Threshold-based segmentation, MobileNetV2 architecture, single shot MultiBox detector (SSD), and a modified feature pyramid network (FPN) with minimum FPN level from 3 to 2. Building upon the limitations and successes of recent works in the field, the proposed methods aim to enhance the efficiency and the ability to detect meningioma brain tumors using bounding boxes. The image's features were enhanced and contrasted using morphological operations such as dilation and erosion [13]. Thresholding-based segmentation identified the desired tumor [14]. The MobileNetV2-SSD with the FPN model was used as a baseline for object detection, with a modified minimum FPN level from 3 to 2 that can effectively help detect small objects.

2.1. Image dataset acquisition

The proposed methods in this study were based on a well-established brain tumor dataset curated by Cheng [12]. The dataset comprises 3064 T1-weighted contrast-enhanced images obtained from 233 patients. These images depict three distinct forms of brain tumors: meningioma (708 slices), glioma (1,426 slices), and pituitary (930 slices). The images in this dataset have a resolution of 512×512. To address the potential issue of overfitting, data splitting was employed. The process entailed dividing the database into three sets, with

training receiving 80% of the resources, validation 10%, and testing another 10%. This enables an objective assessment of the model's generalization and is vital for its predictive capabilities on unseen data.

2.2. Data pre-processing

Before starting training on the dataset with the objection detection model, a few pre-processing techniques were applied to enhance the MRI images' quality and mitigate all the potential issues that might occur. These techniques included histogram equalization [15], grayscale conversion [16], and the application of a Gaussian filter [17]. Figure 1 illustrates the sequential process of these pre-processing techniques leading up to the object detection phase.

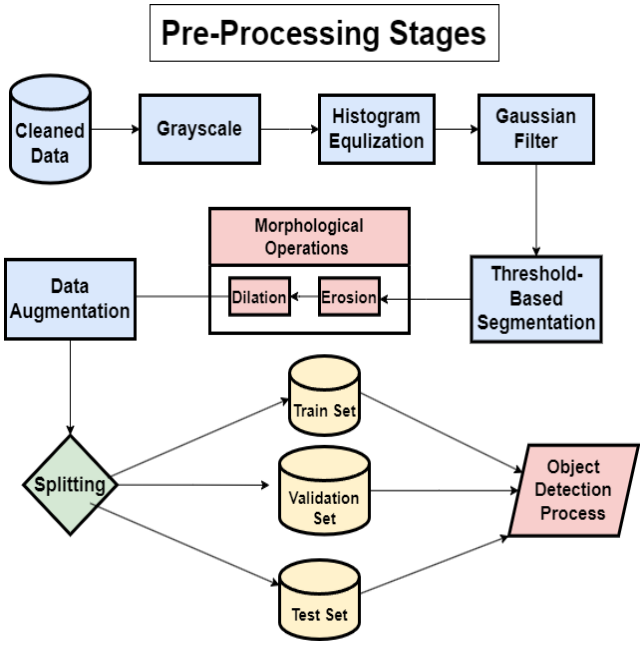

Figure 1. Pre-processing stage flowchart

Prior to proceeding, the images were rendered in greyscale. This transformation simplified the image complexity by representing each pixel with a single integer value, which simplifies computations and is more applicable to certain analysis techniques [18]. Then, histogram equalization was applied, utilizing probability and grey-level calculations to analyze the distribution of grey levels within the image [19], [20]. This technique creates new images with altered distribution and a modified grey level. A Gaussian filter was utilized to filter the image before the segmentation process. This method involves a linear filter with a weighted value for each member. The weighted value is determined by the Gaussian function's shape in (1), where e denotes the normalization constant and σ represents the standard deviation [20].

$$h(x,y) = \frac{1}{c} e^{\frac{x^2+y^2}{2\sigma^2}} \quad (1)$$

2.3. Segmentation

After completing the pre-processing steps of our image, the segmentation step was prepared. A fundamental technique in medical image analysis is threshold-based segmentation, which partitions an image into distinct regions using predetermined threshold values. In the context of grayscale MRI images, thresholding is important because the intensity values span [0, L], with L, often set to 255 for 8-bit grey-scale images [13]. The implementation of the threshold-based approach takes the previous Gaussian-filtered image as an input and sets a threshold value. Utilizing the OpenCV library, binarization was achieved by generating a binary image that highlights brain tumor regions based on intensity variations.

The last step of enhancing the MRI images for object detection was morphological filtering. This technique employs nonlinear operations that utilize a structuring element to probe an image. The operations are based on this element, defining the neighborhood around a pixel and facilitating operations that emphasize or suppress specific features. In this work, two morphological filtering techniques were used:

erosion and dilation [12]. Erosion minimizes pixel values in a window defined by a structuring element, reducing object sizes by eliminating noise. It involves subtracting boundary pixels and gradually decreasing object regions. Dilation enlarges object regions and reduces noise by finding the maximum pixel value in a defined window. In brain tumor segmentation, the predefined kernels for erosion and dilation are used to enhance object regions and suppress background noise.

2.4. Data augmentation

Following pre-processing, data augmentation techniques, which include rotating, width shifting, height shifting, and flipping, were employed to augment the dataset. This process is called data augmentation, which enhances the model's ability to generalize and mitigate the effects of limited data quantity. This approach enriches the training dataset, as emphasized in previous studies by Yang *et al*. [21] and Alomar *et al*. [17].

2.5. Proposed method architecture

In this subsection, the architecture of the proposed experimental model, which comprises several integral components, is defined. These components consist of MobileNetV2, SSD, and feature pyramid network. Additionally, the subsection also discusses the baseline model with the combined components, as well as the proposed experimental model.

2.5.1. MobileNetV2

MobileNetV2, a neural network architecture for computer vision, employs Depthwise convolutions, which apply separate filters to each input channel, reducing computational costs while preserving crucial features. It also utilizes inverted residuals with shortcut connections and linear bottleneck layers to capture intricate details, enhancing accuracy and speed. A lightweight linear bottleneck layer optimizes overall network performance. The architecture of MobileNetV2 in Table 1 shows sequences of identical layers repeated *n* times, with 3×3 spatial convolutions [22]. Every row in the table delineates a sequence consisting of one or more equivalent modulo (denoted as *s)* layers, where it is repeated *n* times, while all layers have the same amount of output channels denoted as *c*. The expansion factor (denoted as *t)* is applied to the input size.

Table 1. MobileNetV2 architecture [22]

Input	Operator	*n*	*t*	*s*	*c*
224×224×3	Conv2d	1	-	2	32
112×112×32	bottleneck	1	1	1	16
112×112×16	bottleneck	2	6	2	24
56×56×24	bottleneck	3	6	2	32
28×28×32	bottleneck	4	6	2	64
14×14×64	bottleneck	3	6	1	96
14×14×96	bottleneck	3	6	2	160
7×7×160	bottleneck	1	6	1	320
7×7×320	Conv2d 1×1	1	-	1	1.280
7×7×1280	Avg pool 7×7	1	-	-	-
1×1×1280	Conv2d 1×1	-	-		k

2.5.2. SSD

A sophisticated object detection model, the single-shot MultiBox detector (SSD), is specifically engineered to accurately detect various object categories within images. Its speed outperforms previous detectors such as YOLO, and its accuracy exceeds that of other methods, such as faster region-based convolutional neural networks (R-CNN). SSD operates by applying small convolutional filters to feature maps in order to forecast category values and box offsets for a predetermined number of default bounding boxes. The training process requires only an input image along with ground truth frames for each object [23]. The SSD network structure is shown in Figure 2(a).

2.5.3. Feature pyramid network

Feature pyramid networks (FPNs) generate a pyramid of feature maps within a neural network, capturing various abstraction levels from the input image. Deeper layers contain high-level semantic information, while shallow layers capture detailed, low-level features. FPN connects these layers to create a multi-scale feature pyramid. Shallow, high-resolution feature maps are up-sampled and fused with deep, high-level feature maps through lateral connections, enhancing detection accuracy for small objects [24]. Figure 2(b) illustrates the pyramid's construction and lateral connection.

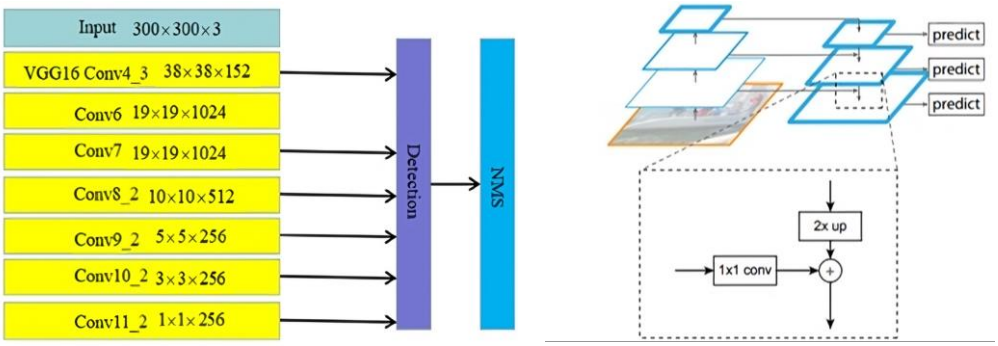

Figure 2. Integrated architecture components of (a) SSD architecture [25] and (b) feature pyramid network illustration [26]

2.5.4. Proposed model

MobileNetV2, a lightweight and efficient neural network, serves as the backbone. It utilizes Depthwise convolutions and inverted residuals for computational efficiency and accuracy. SSD predicts object classes and bounding box offsets using default bounding boxes at various scales and aspect ratios. MobileNetV2's feature maps are employed for object class and location predictions. Integration with feature pyramid network (FPN) enhances detection accuracy for small objects. The baseline model was then optimized by adjusting the FPN configuration. The minimum FPN level was lowered from 3 to 2, starting the feature pyramid network at a shallower layer, specifically layer 4, instead of the default layer 7. This modification aimed to improve the model's precision in detecting and localizing smaller objects in the brain tumor image dataset. Figure 3 shows both the baseline and modified models. Figure 3(a) illustrates the baseline model without the modified FPN layer, whereas Figure 3(b) illustrates the modified model with a reduced FPN level from 3 to 2.

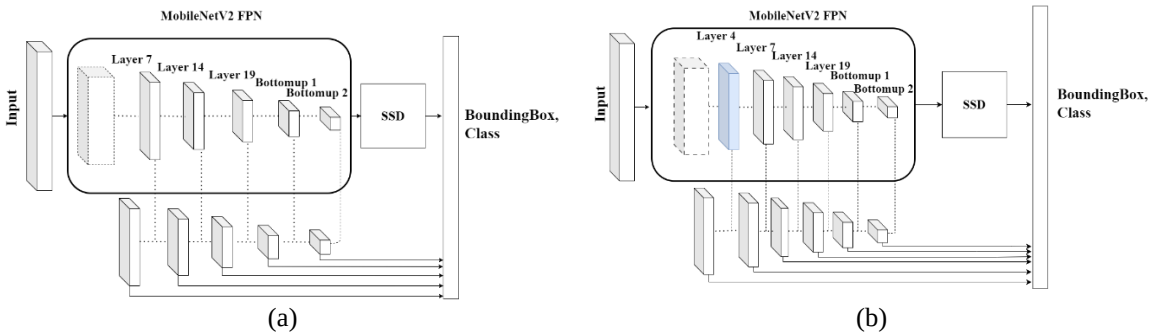

Figure 3. Baseline model architecture and modified model of (a) normal model and (b) experimental model

3. RESULTS AND DISCUSSION

Section 3 focuses on the analysis of performance metrics and measurements, providing a comprehensive evaluation of the experimental model's effectiveness. Following that, a comparison of the testing results from both the normal model and the experimental model is illustrated. Finally, a visual and statistical comparison of the normal model and the experimental model is presented.

3.1. Performance metrics

Below are the two important performance metrics that are used as the testing and the evaluation metric. These performance metrics include average precision (AP) and the coco metrics evaluation. These metrics can determine how effective the experimental model is.

3.1.1. Average precision

AP was used as the evaluation metric, representing the area under the precision-recall (P-R) curve. true positive (TP) represents the count of samples that have been accurately predicted as positive. False

positive (FP) signifies the count of negative samples that have been incorrectly predicted as positive. False negative (FN) represents the count of negative samples that have been incorrectly predicted as positive [13]. Calculation of AP, precision, and recall are shown in (2) to (4), respectively.

$$AP = \int_0^1 P(R)dR \tag{2}$$

$$P = \frac{TP}{TP + FP} \tag{3}$$

$$P = \frac{TP}{TP + FP} \tag{4}$$

3.1.2. Coco metrics evaluation

The second evaluation index employed the common objects in context (COCO) metrics. These metrics encompass a range of intersection over union (IOU) thresholds, including 0.5, 0.75, and the range 0.5:0.95. These thresholds can enable the evaluation of the overlap for both the predicted bounding boxes and the ground truth annotations [25].

3.2. Performance measurement

In subsection 3.2, the process of data splitting is reiterated. Following this initial step, the dataset was partitioned into different subsets, around 80% for training, 10% for validation, and the last 10% for testing purposes. The training set is used, and Figure 4 shows a visualization of the training results per 1,000 steps.

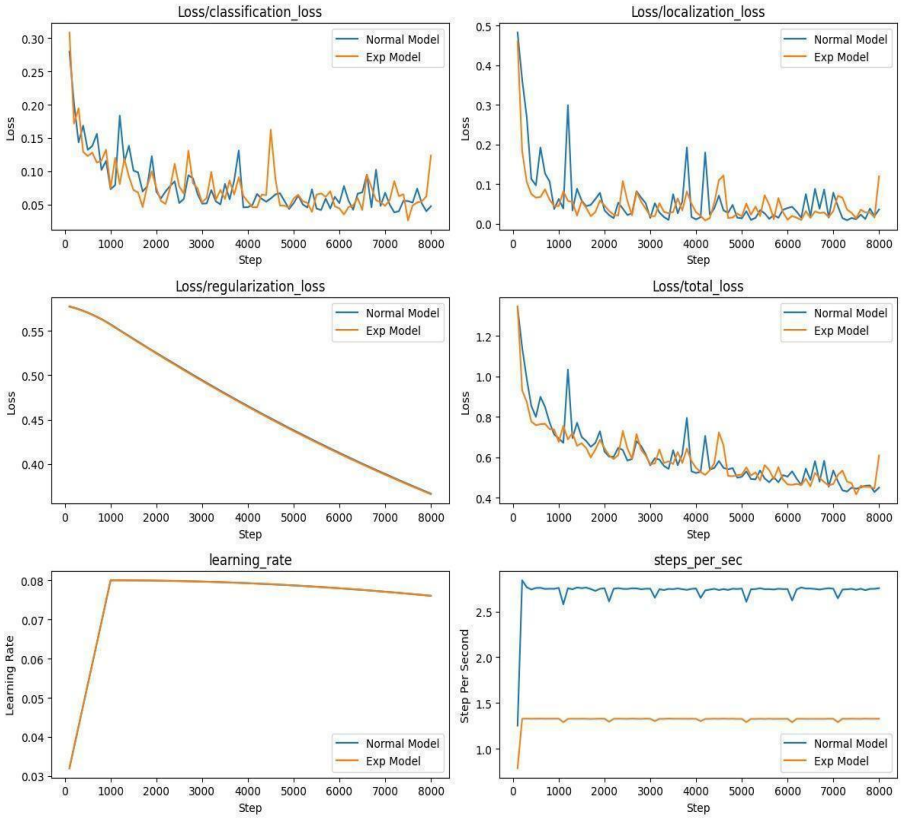

Figure 4. Training performance visualized per 1,000 steps

3.3. Testing results

In this section, the testing results of the proposed MobileNetV2-SSD architecture for brain tumor detection using the modified feature pyramid network (FPN) are presented in Figure 5. The normal model was the baseline model without the modified FPN layer, while the experimental model had a minimized FPN

level from 3 to 2. Each set of results consisted of two images displaying the same brain tumor, with the normal model's predictions on the left and the experimental model's predictions on the right. Ground truth annotations are denoted in green, while the model predictions are indicated in blue. From these results, it is clear that the experimental model exceeds the performance of the normal model, especially in detecting small objects within brain tumor images. The experimental model showcases better localization accuracy, which is indicated by the higher intersection over union (IoU) levels. The visual and statistical comparison between the experimental model and the normal model using a bar chart is illustrated in Figure 6. This chart focuses on average precision (AP) and average recall (AR) values related to detecting smaller objects. In this context, the experimental approach demonstrates remarkable performance, exhibiting substantially higher AP and AR values when compared to the normal model. This shows the experimental model's expertise in precisely identifying and outlining smaller brain tumor regions.

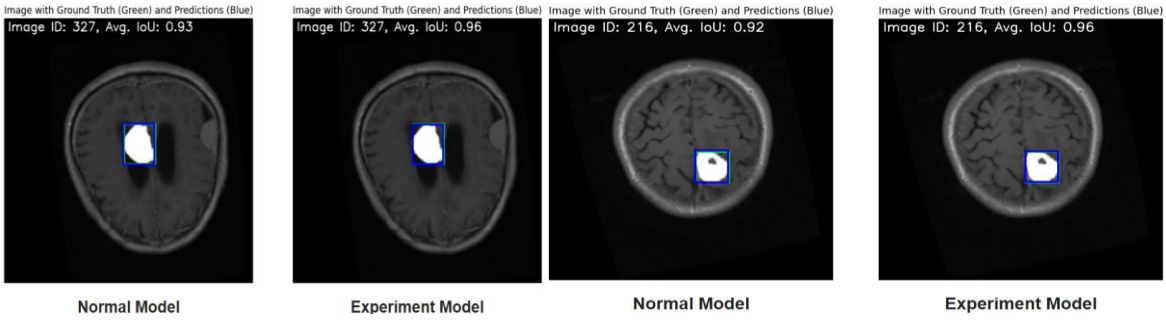

Figure 5. Testing results with both normal model and experimental model outputs. The blue square represents the model's localization predictions, while the green one represents the ground truth annotations

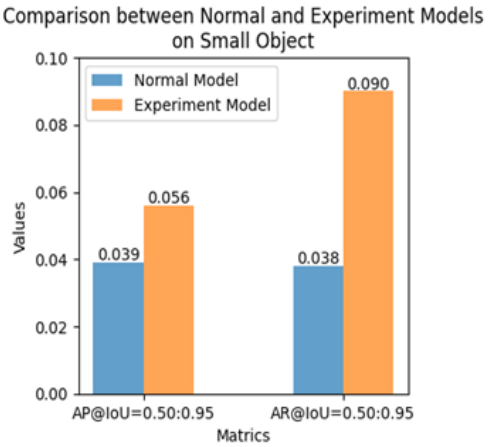

Figure 6. AP and AR comparison on small objects

A comparison of the proposed model with previous research is displayed in Table 2. Previous research obtaining the best performance in terms of precision and recall values was conducted by [10], [26]–[28]. The proposed model in this study by comparison obtained the highest recall value of around 98%, and precision around 89%. Additionally, the proposed model also achieved approximately 93% on both the dice similarity coefficient (DSC) value and the similarity index.

The model proposed in this research focuses on brain tumor localization using MobileNetV2-SSD with minimized FPN level. Table 2 illustrates the evaluation and comparison of the proposed model with the current state-of-the-art models identified in the literature. This experiment results indicated that the performance of the proposed method outperformed other methods, obtaining the highest recall value.

Previously, Saeedi *et al.* [27] utilized k-nearest neighbors (KNN) for brain tumor localization with good performance. However, high computational resources were required due to the utilization of deep networks. Conversely, our proposed model utilized transfer learning, leveraging pre-trained models, which resulted in better performance with minimal complexity.

Swati *et al*. [9] utilized both AlexNet and VGG16 for brain tumor detection with great performance. However, both models were computationally expensive and resource-intensive, hindering their practical deployment. Conversely, our proposed model utilized MobileNetV2, which surpasses AlexNet and VGG16 in terms of efficiency and computational performance due to its lightweight architecture.

Another study conducted by Asif *et al*. [29] utilized Xception, NasNet Large, and DenseNet121 for brain tumor detection. However, a limitation of their study was the lack of tumor localization using bounding boxes. In contrast, our approach employs SSD to address this limitation. Furthermore, SSD combines localization and classification within a unified network, streamlining the training process and mitigating the necessity for extensive labelled data, in contrast to other studies such as Rasool *et al*. [26] and Khan *et al*. [28].

In contrast to Sandrawi *et al.* study [10], which employed readily apparent images, our research concentrates on utilizing smaller and more intricate images to achieve robust detection. Furthermore, the inclusion of FPN, a technique also used by He *et al*. [11], aims to detect subtle tumor features within smaller images. Notably, the experimentation involved the use of a brain tumor dataset for model testing instead.

Nonetheless, this research is not without its limitations. To begin with, our methodology has been exclusively applied to brain tumor images with an axial angle, limiting its applicability to other perspectives. Additionally, while our approach has shown promising results in controlled experimental settings on a limited dataset, it has yet to be tested in real-world clinical environments. Lastly, we utilized the meningioma dataset in our studies. Future research could explore performance optimization and additional evaluation metrics to further enhance and refine this study to provide a more comprehensive understanding of the model's capabilities.

Table 2. Comparative analysis of proposed work with previous works

Ref.	Method	Dataset	Performance Metrics			
			Precision	Recall	DSC	Similarity Index
[9]	AlexNet	Jun Cheng [12]	84.56%	-	-	-
	VGG 16		87.97%	89.98%	-	-
[26]	Hybrid CNN-based		85.1%	94.7%	-	-
[27]	KNN		93%	80%	-	-
[28]	VGG 16 (23 layer)		93.3%	93.3%	-	-
[29]	Xception		87.5%	-	-	-
	NasNet Large		90%	-	-	-
	DenseNet121		89.6%	-	-	-
Proposed Model	MobileNetV2+FPN+SSD		89%	98%	93%	93%

4. CONCLUSION

This study introduced a novel approach for precise brain tumor detection, combining various approaches such as morphological operations for tumor segmentation, image enhancement, and a deep learning architecture based on MobileNetV2-SSD with feature pyramid network (FPN), where the FPN level originally set to 3 had been modified to level 2, which enhanced the detection of smaller objects. The proposed model obtained a recall value of around 98% and a precision value of around 89%. Additionally, the proposed model achieved approximately 93% on the DSC value and the similarity index. Our research achieved significant advancements in the focus of medical imaging based on the promising results. The experimental model recorded the best recall values and high precision, DSC, and similarity index values compared to the previous approaches. It is believed that this work can also be refined by exploring performance optimization methods and different evaluation metrics.

REFERENCES

[1] "Statistics on brain cancer," *World Health Organization*. Accessed: Jul. 01, 2023. [Online]. Available: http://www.who.int/cancer/en/.

[2] A. Kabir Anaraki, M. Ayati, and F. Kazemi, "Magnetic resonance imaging-based brain tumor grades classification and grading via convolutional neural networks and genetic algorithms," *Biocybernetics and Biomedical Engineering*, vol. 39, no. 1, pp. 63–74, Jan. 2019, doi: 10.1016/j.bbe.2018.10.004.

[3] M. Ayyannan, A. Mohanarathinam, D. Sathya, T. Nithya, M. Tamilnidhi, and N. S. Kumar, "Medical image classification using deep learning techniques: a review," in *Proceedings of the 2023 2nd International Conference on Electronics and Renewable Systems*, Mar. 2023, pp. 1327–1332, doi: 10.1109/ICEARS56392.2023.10084948.

[4] B. S. Shukur and M. M. Mijwil, "Involving machine learning techniques in heart disease diagnosis: a performance analysis," *International Journal of Electrical and Computer Engineering (IJECE)*, vol. 13, no. 2, pp. 2177–2185, Apr. 2023, doi: 10.11591/ijece.v13i2.pp2177-2185.

[5] Y. Bhanothu, A. Kamalakannan, and G. Rajamanickam, "Detection and classification of brain tumor in MRI images using deep convolutional network," in *2020 6th International Conference on Advanced Computing and Communication Systems*, Mar. 2020, pp. 248–252, doi: 10.1109/ICACCS48705.2020.9074375.

[6] Q. T. Ostrom, S. S. Francis, and J. S. Barnholtz-Sloan, "Epidemiology of brain and other CNS tumors," *Current Neurology and Neuroscience Reports*, vol. 21, no. 12, Nov. 2021, doi: 10.1007/s11910-021-01152-9.
[7] N. P. Firdi, T. A. Sardjono, and N. F. Hikmah, "Using pectoral muscle removers in mammographic image process to improve accuracy in breast cancer," *Journal of Biomimetics, Biomaterials and Biomedical Engineering*, vol. 55, pp. 131–142, Mar. 2022, doi: 10.4028/p-35cy9o.
[8] A. Khosravanian, M. Rahmanimanesh, P. Keshavarzi, and S. Mozaffari, "Fast level set method for glioma brain tumor segmentation based on superpixel fuzzy clustering and lattice Boltzmann method," *Computer Methods and Programs in Biomedicine*, vol. 198, Jan. 2021, doi: 10.1016/j.cmpb.2020.105809.
[9] Z. N. K. Swati *et al.*, "Brain tumor classification for MR images using transfer learning and fine-tuning," *Computerized Medical Imaging and Graphics*, vol. 75, pp. 34–46, Jul. 2019, doi: 10.1016/j.compmedimag.2019.05.001.
[10] M. Sadrawi, D. R. Fugaha, D. M. Heerlie, J. Lorell, N. R. P. Gautama, and M. Z. Aminuddin, "Artificial intelligence based brain tumor localization using YOLOv5," *Indonesian Journal of Life Sciences*, pp. 1–9, Mar. 2023, doi: 10.54250/ijls.v5i01.176.
[11] J. He, J. Wang, Z. Han, B. Li, M. Lv, and Y. Shi, "Cancer detection for small-size and ambiguous tumors based on semantic FPN and transformer," *PLoS ONE*, vol. 18, Feb. 2023, doi: 10.1371/journal.pone.0275194.
[12] J. Cheng, "Brain tumor dataset," 2017. https://doi.org/10.6084/m9.figshare.1512427.v5 (accessed Jan. 03, 2023).
[13] P. R. Kumar and S. S. Marthurkar, "A review on morphological filter and its implementation," *International Journal of Science and Research (IJSR)*, vol. 6, no. 1, pp. 69–72, Jan. 2017, doi: 10.21275/art20163953.
[14] U. Chandra De, M. Das, D. Mishra, and D. Mishra, "Threshold based brain tumor image segmentation," *International Journal of Engineering and Technology*, vol. 7, no. 3, Aug. 2018, doi: 10.14419/ijet.v7i3.12425.
[15] M. Ben naceur, M. Akil, R. Saouli, and R. Kachouri, "Fully automatic brain tumor segmentation with deep learning-based selective attention using overlapping patches and multi-class weighted cross-entropy," *Medical Image Analysis*, vol. 63, Jul. 2020, doi: 10.1016/j.media.2020.101692.
[16] J. Cheng *et al.*, "Correction: enhanced performance of brain tumor classification via tumor region augmentation and partition," *PLOS ONE*, vol. 10, no. 12, p. e0144479, Dec. 2015, doi: 10.1371/journal.pone.0144479.
[17] K. Alomar, H. I. Aysel, and X. Cai, "Data augmentation in classification and segmentation: a survey and new strategies," *Journal of Imaging*, vol. 9, no. 2, Feb. 2023, doi: 10.3390/jimaging9020046.
[18] A. Bugeau, R. Giraud, and L. Raad, "Influence of color spaces for deep learning image colorization," in *Handbook of Mathematical Models and Algorithms in Computer Vision and Imaging: Mathematical Imaging and Vision*, Springer International Publishing, 2023, pp. 847–878.
[19] Y. Xie, L. Ning, M. Wang, and C. Li, "Image enhancement based on histogram equalization," *Journal of Physics: Conference Series*, vol. 1314, no. 1, Oct. 2019, doi: 10.1088/1742-6596/1314/1/012161.
[20] Kusrini, M. R. A. Yudianto, and H. Al Fatta, "The effect of Gaussian filter and data preprocessing on the classification of Punakawan puppet images with the convolutional neural network algorithm," *International Journal of Electrical and Computer Engineering (IJECE)*, vol. 12, no. 4, pp. 3752–3761, Aug. 2022, doi: 10.11591/ijece.v12i4.pp3752-3761.
[21] S. Yang, W. Xiao, M. Zhang, S. Guo, J. Zhao, and F. Shen, "Image data augmentation for deep learning: a survey," Apr. 2022, [Online]. Available: http://arxiv.org/abs/2204.08610.
[22] M. Sandler, A. Howard, M. Zhu, A. Zhmoginov, and L.-C. Chen, "MobileNetV2: inverted residuals and linear bottlenecks," in *2018 IEEE/CVF Conference on Computer Vision and Pattern Recognition*, Jun. 2018, pp. 4510–4520, doi: 10.1109/CVPR.2018.00474.
[23] W. Liu *et al.*, "SSD: Single Shot MultiBox Detector," in *Lecture Notes in Computer Science (including subseries Lecture Notes in Artificial Intelligence and Lecture Notes in Bioinformatics)*, 2016, pp. 21–37.
[24] T.-Y. Lin, P. Dollar, R. Girshick, K. He, B. Hariharan, and S. Belongie, "Feature pyramid networks for object detection," in *2017 IEEE Conference on Computer Vision and Pattern Recognition (CVPR)*, Jul. 2017, pp. 936–944, doi: 10.1109/CVPR.2017.106.
[25] Naseer-U-Din, A. Basit, I. Ullah, W. Noor, A. Ahmed, and N. Sheikh, "Brain tumor detection in MRI scans using single shot multibox detector," *Journal of Intelligent and Fuzzy Systems*, vol. 43, no. 2, pp. 1985–1993, Jun. 2022, doi: 10.3233/JIFS-219298.
[26] M. Rasool *et al.*, "A hybrid deep learning model for brain tumour classification," *Entropy*, vol. 24, no. 6, Jun. 2022, doi: 10.3390/e24060799.
[27] S. Saeedi, S. Rezayi, H. Keshavarz, and S. R. Niakan Kalhori, "MRI-based brain tumor detection using convolutional deep learning methods and chosen machine learning techniques," *BMC Medical Informatics and Decision Making*, vol. 23, no. 1, Jan. 2023, doi: 10.1186/s12911-023-02114-6.
[28] M. S. I. Khan *et al.*, "Accurate brain tumor detection using deep convolutional neural network," *Computational and Structural Biotechnology Journal*, vol. 20, pp. 4733–4745, 2022, doi: 10.1016/j.csbj.2022.08.039.
[29] S. Asif, W. Yi, Q. U. Ain, J. Hou, T. Yi, and J. Si, "Improving effectiveness of different deep transfer learning-based models for detecting brain tumors from MR images," *IEEE Access*, vol. 10, pp. 34716–34730, 2022, doi: 10.1109/ACCESS.2022.3153306.

BIOGRAPHIES OF AUTHORS

Nada Fitrieyatul Hikmah earned her bachelor's degree in biomedical engineering from Airlangga University (UNAIR) in 2012 and her master's education in electrical engineering electronics, specializing in biomedical engineering, at the Sepuluh Nopember Institute of Technology (ITS) in 2016. Currently, she works as a lecturer at the Department of Biomedical Engineering, Faculty of Electrical Technology and Intelligent Informatics, ITS, Indonesia. Her research interests include cardiac engineering, signal processing, and medical imaging. She can be contacted at email: nadafh@bme.its.ac.id.

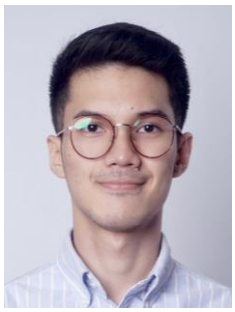

Ariq Dreiki Hajjanto is a final year undergraduate student majoring in biomedical engineering at Sepuluh Nopember Institute of Technology in Surabaya, Indonesia. His academic journey began in 2020, and since then, he has actively immersed himself in both studies and research endeavors. Currently, he serves as a research assistant at the Research Center for Metallurgy within the National Research and Innovation Agency in Indonesia. His primary expertise lies in medical imaging, where he applies computational techniques to enhance and analyze biomedical images. He can be contacted at email: Ariqdreiki213@gmail.com.

Armand Faris A. Surbakti is a final year undergraduate biomedical engineering student who enrolled in the year 2020 at Sepuluh Nopember Institute of Technology, Surabaya, Indonesia. He is currently a research assistant in the Research Center for Metallurgy, Nation Research and Innovation Agency, Indonesia. His research interest is medical informatics, which is the field of combining medical practices with information technology, which consists of integrating deep learning for medical purposes, creating websites for medical organizations, and developing mobile applications for health development and research. He can be contacted at email: 5023201051@student.its.ac.id.

Nadhira Anindyafitri Prakosa is a final year undergraduate biomedical engineering student at Sepuluh Nopember Institute of Technology, Surabaya, Indonesia. She began her academic journey in the year 2020 and has since been actively engaged in her studies and research pursuits. Currently, she is a research assistant at the Research Center for Metallurgy within the National Research and Innovation Agency in Indonesia. Her primary interest lies in medical imaging, where she employs computational techniques to enhance and analyze biomedical images. She can be contacted at email: prakosanadhiraap@gmail.com.

Talitha Asmaria received a bachelor of engineering in biomedical engineering major in 2012 from Airlangga University, Surabaya, Indonesia. She has completed her MSc degree in 2016 from biomedical engineering at the University of Bristol, United Kingdom. She is currently an early career researcher in the Center of Biomedical Research, Organization of Health, National Research and Innovation Agency (BRIN), Indonesia, and a lecturer in the biomedical engineering study program, International University of Liaison Indonesia. Her research interest is the implant planning, which includes design analysis, image processing, material development, and 3D printing technology. She can be contacted at email: talitha.asmaria@brin.go.id.

Tri Arief Sardjono earned his bachelor's degree in electrical engineering from the Sepuluh Nopember Institute of Technology (ITS), Indonesia, in 1994 and his master's degree in the field of informatics engineering from the Bandung Institute of Technology (ITB) in 1999. He received Ph.D. in biomedical engineering at the University of Groningen, Netherlands, and earned his doctoral degree in 2008. Currently, he works as a lecturer at the Department of Biomedical Engineering, Faculty of Electrical Technology and Intelligent Informatics, ITS. His research interests encompass medical imaging, ultrasound imaging and analysis. He can be contacted at email: sardjono@bme.its.ac.id.